

## ARTICLE



# Quantitative analysis of preclinical ocular microvascular changes in Multisystemic Inflammatory Syndrome in Children (MIS-C) detected by optical coherence tomography angiography

Büşra Yılmaz Tuğan<sup>1</sup> , Hafize Emine Sönmez<sup>2</sup>, Kübra Atay<sup>1</sup>, Eviç Zeynep Başar<sup>3</sup>, Berna Özkan<sup>4</sup> and Levent Karabaş<sup>1</sup>

© The Author(s), under exclusive licence to The Royal College of Ophthalmologists 2022

**OBJECTIVES:** To evaluate the macular and optic nerve head (ONH) vascular density, foveal avascular zone area, and outer retina and choriocapillaris flow in Multisystemic Inflammatory Syndrome in Children (MIS-C) using optical coherence tomography angiography (OCTA).

**METHODS:** Thirty-four eyes of 34 patients with MIS-C and 36 age and sex-matched healthy controls were investigated in this prospective, cross-sectional study. The superficial capillary plexus (SCP) and deep capillary plexus (DCP), ONH, FAZ parameters, the flow area of the outer retina, and choriocapillaris were evaluated using OCTA.

**RESULTS:** All VD parameters in SCP were significantly lower in MIS-C patients. There was no significant difference between the groups in VD parameters of both DCP and ONH, as well as FAZ area and FAZ perimeter. However, foveal density (FD-300) was significantly decreased in the MIS-C group. ( $p = 0.024$ ). The outer retina flow area at 1 mm, 2 mm, and 3 mm radius and CC flow area at 1 mm and 2 mm radius were significantly lower in the MIS-C group than in the control group. Although CC flow area at 3 mm radius was decreased in the MIS-C group compared to healthy controls, the difference was not statistically significant.

**CONCLUSIONS:** We demonstrated a decreased vessel density in SCP, choriocapillaris flow area, and outer retinal flow area in MIS-C patients. Hence, we proposed that OCTA could reveal retinal and choroidal microvascular changes in MIS-C patients who were completely healthy before the diagnosis of MIS-C.

Eye; <https://doi.org/10.1038/s41433-022-02081-8>

## INTRODUCTION

Multisystemic Inflammatory Syndrome in Children (MIS-C) emerged as a new disorder after the pandemic of SARS-CoV-2 infection [1]. It is a post-acute inflammatory illness that often presents 4–5 weeks on average after SARS-CoV-2 exposure. A cytokine storm leading to tissue injury is suggested as the underlying aetiology while the data enlightening specific pathophysiology has not been determined yet [2]. Initial reports defined this new condition as Kawasaki-like disease. However, it is well known now that the spectrum of disease has expanded with varying systemic involvement, including ocular manifestations. Conjunctivitis is the most common ocular feature seen in almost half of MIS-C patients [3], while the effect of the disease on the retina has not been elucidated yet. Microvascular damage and endothelial injury have been determined among patients with MIS-C [4]. Therefore, retinal vessels may be a target in the course of the disease.

Optical coherence tomography angiography (OCT-A) enables a non-invasive evaluation of retinal microvasculature that exceeds the capability of other forms of imaging [5]. OCTA can quantify superficial (SCP) and deep capillary plexus (DCP), peripapillary

region, choriocapillaris (CC), and outer retina, separately. OCTA also provides information about the shape and dimensions of the foveal avascular zone (FAZ) [6]. Thus, impaired systemic microcirculation might be mapped on the retinal capillary system. Previous studies evaluating the retinal vessel density changes related to COVID-19 infection yielded different results [7–9].

To the best of our knowledge, there have been no published studies assessing the state of the retinal microvasculature in patients after SARS-CoV-2 related MIS-C. The main objective of the present cross-sectional study was to perform not only a direct retinal observation but an in-depth analysis of the retinal vascular plexuses and flow to detect possible subclinical retinal vascular involvement associated with the prothrombotic and hyperinflammatory state in MIS-C.

## METHODS

### Participants

This prospective observational study was performed from March 2021 to June 2021. The study protocol was approved by the Ethics Committee at

<sup>1</sup>Kocaeli University, Department of Ophthalmology, Kocaeli, Turkey. <sup>2</sup>Kocaeli University, Division of Pediatrics, Department of Pediatric Rheumatology, Kocaeli, Turkey. <sup>3</sup>Kocaeli University, Division of Pediatrics, Department of Pediatric Cardiology, Kocaeli, Turkey. <sup>4</sup>Acibadem Mehmet Ali Aydınlar University, Department of Ophthalmology, İstanbul, Turkey. ✉email: busrayilmaz87@hotmail.com

Received: 8 October 2021 Revised: 1 April 2022 Accepted: 22 April 2022

Published online: 29 April 2022

Kocaeli University and adhered to the principles of the Declaration of Helsinki. Informed consent was obtained from all participants.

To determine the sample size, power analysis was performed by G\*Power program for effect size = 0.8;  $\alpha = 0.05$  and power  $(1-\beta) = 0.80$ . Sample size was calculated as 26 eyes for each of the MIS-C and control groups. Thirty-four eyes of 34 paediatric patients were diagnosed with MIS-C according to the diagnostic criteria of CDC and WHO [10, 11]. The control group consisted of 36 eyes of 36 age and sex-matched healthy peers without a prior history of ocular or systemic diseases admitted to our ophthalmology clinic for refractive spherical or cylindrical error  $< 2$  D with BCVA of  $\geq 20/20$  and no other ocular or systemic diseases. Data were collected from the right eye of each participant. Clinical and laboratory findings, outcomes, and additional treatments were obtained from the medical charts of the patients.

Exclusion criteria for both groups were best-corrected visual acuity (BCVA)  $< 20/20$ , active or previous uveitis findings, any pathology on biomicroscopic and fundus examination, any retinal and choroidal pathology observed on optical coherence tomography (OCT) of the macula, and enhanced-depth imaging (EDI) OCT of the choroid and any other systemic disease.

### Examination protocol

All participants underwent routine ophthalmic evaluation including BCVA, slit-lamp biomicroscopy, IOP measurement with Goldmann applanation tonometry, axial eye length (AL) measurement using an IOLMaster (ver. 3.02; Carl Zeiss, Meditec, Jena, Germany), central corneal thickness (CCT) with a full auto tonometer (Canon TX-20P, Tokyo, Japan), spherical equivalent (SE formula = Cylindrical power/2 + Spherical power). After pupillary dilatation, fundus examination, retinal nerve fibre layer thickness (RNFL), central macular thickness (CMT), subfoveal choroidal thickness (CT) by SD-OCT (Heidelberg Engineering GmbH, Heidelberg, Germany), and Optical Coherence Tomography Angiography (OCTA) were performed.

### OCTA assessment

In the current study, the Optovue AngioVue system (RTVue XR Avanti; Optovue Inc., Fremont, CA, USA) was used for evaluating the macular, optic nerve head (ONH), and foveal avascular zone (FAZ) regions. Optovue AngioVue system is an angiographic programme that includes an SD-OCT providing both thickness and vascular density, flow, and non-flow parameters.

$6 \times 6$  mm protocol of density assessment tool was performed to assess the macular region to cover the whole macular region in both superficial capillary plexus (SCP) and deep capillary plexus (DCP). The internal software (Optovue Inc., software version: 2018.0.0.14) measured the whole-image vessel density (VD), the parafoveal VD (centred on the fovea from 1 mm diameter to 3 mm diameter), and perifoveal VD (centred on the parafovea from 3 mm diameter to 6 mm diameter). Furthermore, the parafoveal and perifoveal areas were subdivided into four equal size quadrants (temporal, nasal, inferior, and superior) and two equal size hemispheres (superior and inferior) (Fig. 1A–F).

$4.5 \times 4.5$  mm protocol of density assessment tool was performed to assess the optic nerve head (ONH). ONH-centred annular region of interest (ROI) was over-imposed onto the peripapillary OCTA scan. Internal software calculates total (whole image), peripapillary, and inside disc VD automatically (Fig. 1G–I).

FAZ assessment tool was used to obtain the area of FAZ in full retinal vasculature ( $\mu\text{m}^2$ ), the perimeter of FAZ ( $\mu\text{m}$ ) and foveal density-300  $\mu\text{m}$  (FD-300) (vessel density within a 300  $\mu\text{m}$  ring surrounding the FAZ) (Fig. 2A–C). The FAZ area ( $\mu\text{m}^2$ ) in SCP was evaluated using the non-flow assessment tool (Fig. 2D–F). Outer retina and choriocapillaris flow area centred on FAZ at 1 mm, 2 mm, and 3 mm was obtained via flow assessment tool (Fig. 3).

Poor-quality images with (1) image-quality index  $< 7/10$ , (2) poor clarity, (3) motion or vitreous floater artifacts, and (4) segmentation errors, were not included.

### Statistical analysis

The statistical analysis was carried out using the SPSS software version 21.0. The variables were investigated using visual (histogram, probability plots) and analytic methods (Kolmogorov-Smirnov/Shapiro-Wilk's test) to determine whether or not they are normally distributed. Descriptive statistics were shown as proportions and mean values, whichever was appropriate. The Chi-square test or Fisher's exact test was used to examine

the associations between two categorical variables whichever was appropriate. Independent samples T-test was used to compare the continuous variables between two groups. Pearson test was used to evaluate the associations between variables. The significance was tested at the 5% level and differences were considered statistically significant at  $p \leq 0.05$ .

### RESULTS

A total of 34 patients with MIS-C were evaluated. Among them, 20 were female and 14 were male. Of 34 patients, 30 (88.2%) had a history of contact with COVID-19 patients. At admission, SARS-CoV-2 PCR was negative in all patients, and all were positive for SARS-CoV-2 IgG or IgM. The mean age of patients was  $10.94 \pm 3.08$ . All patients presented with fever lasting 4 [2–7] days. The median time of hospitalization was  $9.12 \pm 2.84$  days. All patients were discharged without sequelae. The mean time between diagnosis and ocular evaluation was  $37.47 \pm 5.18$  days. Age and sex-matched, 36 healthy volunteers were enrolled. Supplementary Table 1 shows the demographic and clinical characteristics of study participants. There were no significant differences in age, sex, IOP, SE, AL, CCT, CMT, subfoveal CT, and RNFL thickness between MIS-C and control groups ( $p > 0.05$  for all). One case in the MIS-C group and one case in the control group were excluded because the image-quality index was  $< 7/10$ . The mean image-quality index for macula was  $8.00 \pm 0.88$  in the MIS-C group and  $7.96 \pm 0.82$  in the normal controls ( $p = 0.861$ ). The mean image-quality index for optic disc was  $8.13 \pm 0.70$  in the MIS-C group and  $7.92 \pm 0.84$  in the normal controls ( $p = 0.335$ ).

### Vessel density evaluation of macular and peripapillary region

Macular and optic nerve head VD parameters of enrolled participants were reported in Table 1. All VD parameters in SCP were significantly decreased in the MIS-C group compared to healthy controls. Also, VD parameters of both DCP and ONH were decreased in the MIS-C group than in the control group, but this difference was not statistically significant ( $p > 0.05$  for all).

### FAZ, Non-flow and flow evaluation

Non-flow, flow, and FAZ parameters of both MIS-C and control groups were presented in Table 2. FAZ area in full retinal vasculature, FAZ perimeter, and FAZ area in SCP did not show any significant changes between the 2 study groups ( $p > 0.05$  for all). However, FD-300 was significantly decreased in MIS-C group ( $p = 0.024$ ).

The outer retina flow area at 1 mm, 2 mm, and 3 mm radius and CC flow area at 1 mm and 2 mm radius were significantly lower in the MIS-C group than in the control group. Although CC flow area at 3 mm was decreased in the MIS-C group compared to healthy controls, the difference did not show statistical significance.

### DISCUSSION

The current study is the first to evaluate the retinal vascular status in a cohort of recovered SARS-CoV-2 related MIS-C patients. In the current study, OCTA was performed to compare the VD of the retinal capillary microvasculature in MIS-C patients versus age and sex-matched healthy controls. The main finding of the study is decreased VD in SCP and decreased flow in outer retina and choriocapillaris layer related to MIS-C.

However, the exact effect of SARS-CoV-2 on microvascular circulation has not been clarified yet, initial reports showed that endothelial injury and microvascular damage act as the originator of systemic inflammation and thrombosis in severe COVID-19 [12–14]. Since COVID-19 causes endothelial damage, the impact of COVID-19 on retinal and choroidal vasculature has been of interest. In literature, several studies regarding macular region VD in adult recovered COVID-19 patients yielded different results



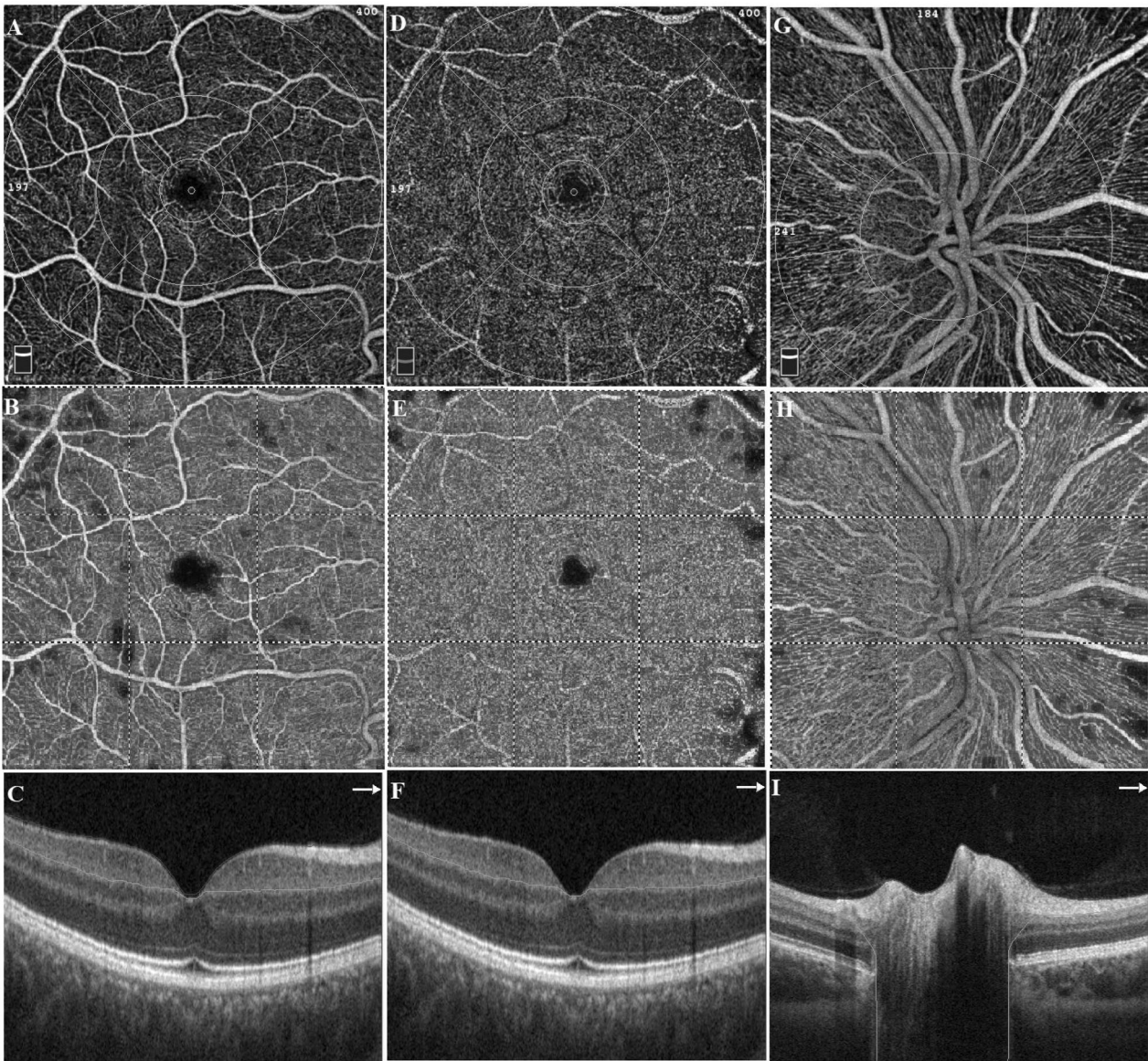


**Fig. 1** *Density measurement of a representative case of MIS-C patients.* ETDRS rings on macula represent from inside to outside: 1 mm for fovea, 3 mm for parafovea, and 6 mm for perifovea. The SCP (A) is automatically segmented by the software from the inner limiting membrane (ILM) (red line) to the inner plexiform layer (IPL) (green line) (C). B Colour image of the superficial macular region. The DCP (D) is automatically segmented by the software from the IPL (green line) to the outer plexiform layer (OPL) (red line) (F). E Colour image of the deep macular region. VD of the optic nerve head (ONH) (G) is automatically segmented by the software from the ILM (red line) to the nerve fibre layer (NFL) (green line) (I). H The rings represent total, inside disc and peripapillary VD in  $4.5 \times 4.5$  mm scan size. Colour image of the peripapillary region.

[8, 9]. In Abrishami et al. [8] study, mean macular superficial and deep capillary plexus VD were significantly reduced in the COVID-19 patients compared to the age-matched controls. In Savastano et al. [7] study, the authors evaluated post-COVID-19 patients one month after discharge from the hospital. They revealed no significant difference in SCP and DCP in the COVID-19 group compared to the control group even after performing binary logistic regression analysis to exclude confounding factors [7]. In another study evaluating macular microcirculation at three capillary layers as SCP, intermediate capillary plexus (ICP), and DCP, authors reported that overall macula VD of the SCP and DCP was not significantly different between post-COVID patients and controls, but VD of ICP was significantly lower in post-COVID patients compared to controls [9]. Zapata et al. [15] stratified patients as mild, moderate, and severe according to disease severity. They concluded that fovea-centred VD was significantly lower in the moderate and severe patient groups compared to the

mild patient group and control group [15]. Turker et al. [16] examined recovered COVID-19 patients at an early period and 6 months. They reported a decrease in VD values in all parafoveal quadrants of the SCP and DCP in the early period and also in all parafoveal quadrants of the SCP and 2 (superior, inferior) of the parafoveal quadrants of the DCP at 6-months after COVID-19 infection. Yet they did not find a significant difference regarding SCP and DCP VD between the patient group and the control group at either the early period or 6-month after COVID-19 infection [16]. In the current study, we demonstrated decreased VD parameters in MIS-C patients even after the mean time of  $37.47 \pm 5.18$  days between MIS-C diagnosis and ocular examination. Cennamo et al. [17] reported that all macular DCP parameters showed significant reduction but only whole image VD in SCP was decreased in the COVID-19 group compared to the controls. Conversely, in one study, the authors revealed that SCP was affected more than DCP. While significantly lower foveal and



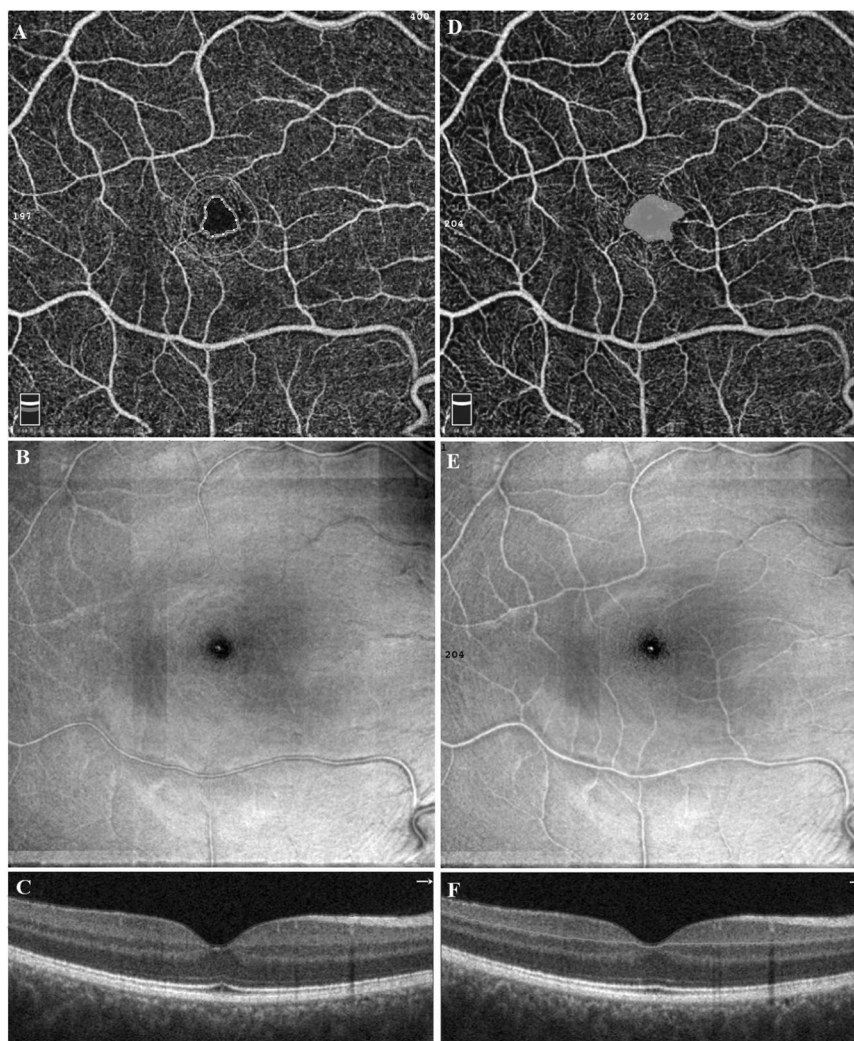


**Fig. 2** FAZ, and non-flow measurement of a representative case of MIS-C patients. FAZ area ( $\text{mm}^2$ ) in full retinal vasculature, FAZ perimeter (mm), and foveal density-300 (FD) (A) were automatically calculated in the full retinal vasculature and segmented by the software from the ILM (top red line) to the OPL (bottom red line) (C). B C-scan (en-face) image of FAZ area in full retinal vasculature. FAZ area ( $\text{mm}^2$ ) (D) was calculated in SCP and segmented by the software from the ILM (red line) to the IPL (green line) (F). E En-face image of FAZ area in SCP.

parafoveal VD in SCP was observed in COVID-19 patients compared to controls, in DCP, only foveal VD was significantly lower in the patient group compared to controls [18].

MIS-C is an emerging disorder that initially presented in the midst of a global pandemic and broke the belief that children are blessed by COVID-19. The underlying pathology in MIS-C patients is thought to be tissue injury secondary to the cytokine storm. Supporting this hypothesis, Fraser et al. [4] demonstrated increased levels of 21 different cytokines related to endothelial injury such as MMP7, IP-10, resistin, and IL-3. However, unlike adult COVID-19 studies, the effect of MIS-C on vasculature in children has not been investigated exhaustively. In the current study, we evaluated the influence of MIS-C on retinal and choroidal microvasculature and we demonstrated a significant decrease of VD in all SCP regions and also outer retina and CC flow in the MIS-C group with respect to the healthy controls. Therefore, in view of our findings, impaired retinal and choroidal microvasculature may be one of the results of this new emergency phenomenon. Overall, previous studies with OCTA revealed a much more significant decrease of DCP VD than SCP VD in COVID-19 patients compared to controls, as also occurs in diabetic retinopathy and other vascular diseases [19–21]. This entity was attributed to the indirect connection of DCP to arterioles and being more

vulnerable to thrombotic events than SCP. Although, in the present study, we also showed decreased VD parameters in the DCP of MIS-C patients, this difference did not reach statistical significance. A significant reduction was observed in VD parameters of SCP in the MIS-C patients compared to the controls. The small number of patients may have caused this difference to be insignificant. Since MIS-C is quite different from the other intense inflammatory syndromes of childhood, further studies with a larger cohort would help us to demonstrate the changes in retinal vascular plexus related to MIS-C.

The previous studies investigated possible changes in VD of the ONH region in COVID-19 patients. In Cennamo et al. [17] study, the authors revealed that whole image ONH VD was significantly lower in COVID-19 patients compared to controls. In that study, no difference was observed in the inside disc and peripapillary VD between the two groups. In another study, lower ONH perfusion density in the post-COVID-19 group compared to the control group was observed [22]. In the current study, no significant differences were found between ONH parameters of MIS-C patients and the controls.

There have been studies comparing FAZ parameters of COVID-19 patients and healthy controls. In Abrishami et al. [8] and Cennamo et al. [17] studies, FAZ area was also greater in the



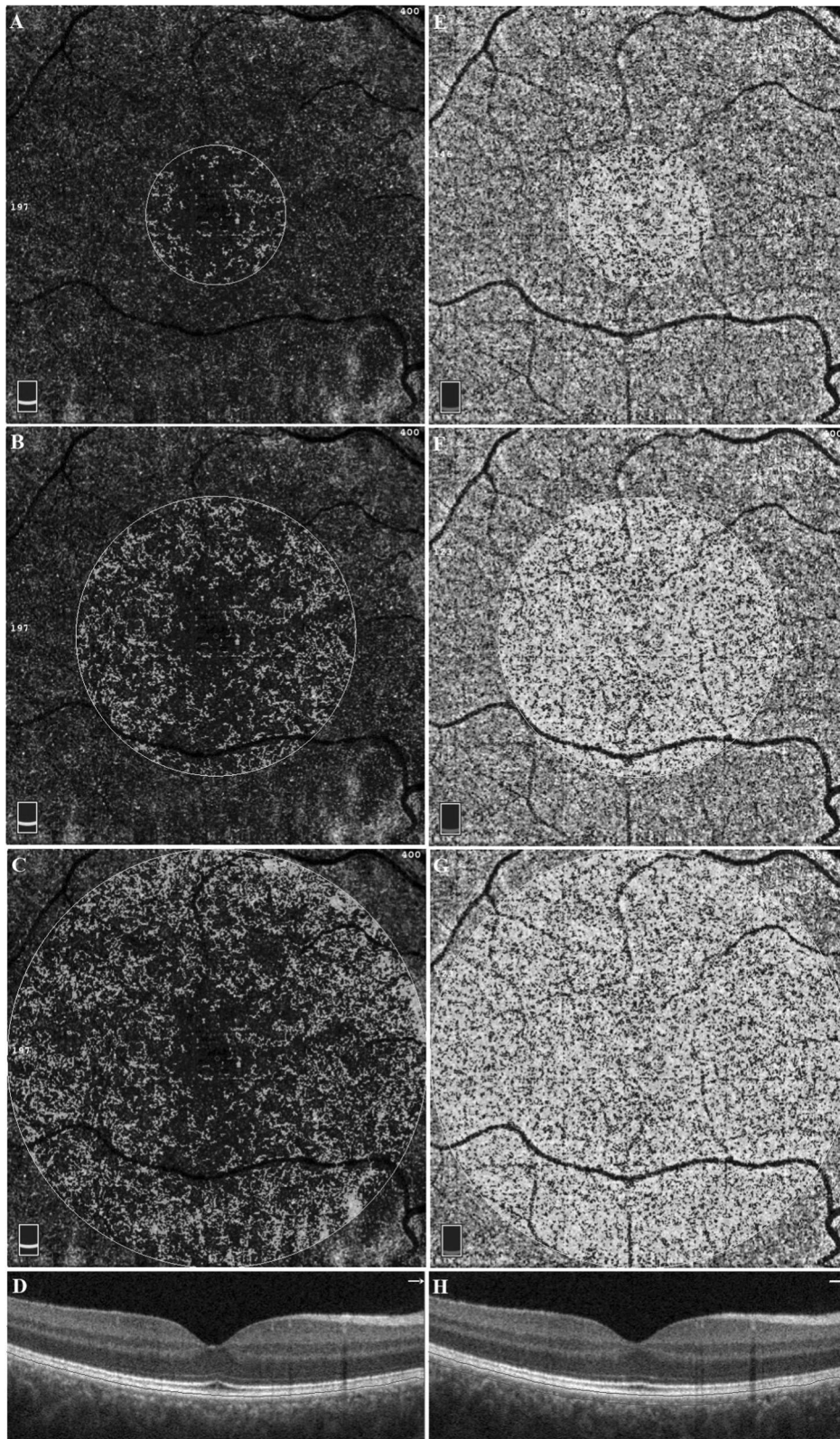


**Fig. 3** Flow measurement of a representative case of MIS-C patients. **A** Flow measurement in the outer retina (left column) calculated at 1 mm, 2 mm (**B**), and 3 mm (**C**) radius. **D** The blood flow was calculated in  $\text{mm}^2$  centred on the fovea in the outer retina layer, segmented automatically from the outer plexiform layer (OPL) and the Bruch membrane (BRM). Flow measurement in the choriocapillaris (right column) calculated at 1 mm (**E**), 2 mm (**F**), and 3 mm (**G**) radius. **H** The blood flow was calculated in  $\text{mm}^2$  centred on the fovea in the choriocapillaris, segmented automatically from BRM to  $30\ \mu\text{m}$  inferiorly to the BRM.

**Table 1.** Macular and Optic Nerve Head Vessel Density Assessment Tool Parameters of OCTA.

|                              | MIS-C group<br>(n = 34)<br>Mean ± SD | Control group<br>(n = 36)<br>Mean ± SD | p*               |
|------------------------------|--------------------------------------|--|------------------|
| <b>VD of SCP (%)</b>         |                                      |  |                  |
| Whole image                  | 49.16 ± 3.75                         | 51.48 ± 2.27                           | <b>0.002</b>     |
| Sup hemi                     | 49.08 ± 3.54                         | 51.58 ± 2.45                           | <b>0.001</b>     |
| Inf hemi                     | 49.26 ± 4.06                         | 51.40 ± 2.29                           | <b>0.011</b>     |
| Fovea                        | 18.86 ± 5.69                         | 21.22 ± 6.53                           | <b>0.021</b>     |
| Parafovea                    | 49.95 ± 6.16                         | 54.21 ± 2.68                           | <b>0.002</b>     |
| Para sup hemi                | 50.35 ± 6.34                         | 54.86 ± 2.54                           | <b>0.001</b>     |
| Para inf hemi                | 49.53 ± 6.39                         | 53.54 ± 3.23                           | <b>0.008</b>     |
| Para superior                | 50.64 ± 6.52                         | 55.42 ± 2.87                           | <b>0.002</b>     |
| Para nasal                   | 49.17 ± 6.26                         | 53.12 ± 3.30                           | <b>0.003</b>     |
| Para inferior                | 49.39 ± 7.07                         | 53.45 ± 4.19                           | <b>0.029</b>     |
| Para temporal                | 50.61 ± 6.06                         | 54.82 ± 2.79                           | <b>&lt;0.001</b> |
| Perifovea                    | 49.87 ± 4.11                         | 52.10 ± 2.29                           | <b>0.004</b>     |
| Peri sup hemi                | 49.89 ± 3.94                         | 52.01 ± 2.53                           | <b>0.004</b>     |
| Peri inf hemi                | 49.86 ± 4.47                         | 52.20 ± 2.35                           | <b>0.007</b>     |
| Peri superior                | 49.81 ± 3.98                         | 52.09 ± 3.27                           | <b>0.007</b>     |
| Peri nasal                   | 53.19 ± 3.78                         | 55.14 ± 2.37                           | <b>0.013</b>     |
| Peri inferior                | 49.94 ± 4.37                         | 51.97 ± 2.79                           | <b>0.039</b>     |
| Peri temporal                | 46.62 ± 5.24                         | 49.17 ± 2.04                           | <b>0.012</b>     |
| <b>VD of DCP (%)</b>         |                                      |  |                  |
| Whole image                  | 52.79 ± 7.12                         | 53.49 ± 5.43                           | 0.422            |
| Sup hemi                     | 51.78 ± 7.48                         | 53.54 ± 5.26                           | 0.290            |
| Inf hemi                     | 52.48 ± 7.02                         | 53.30 ± 5.63                           | 0.508            |
| Fovea                        | 36.94 ± 7.02                         | 38.07 ± 7.30                           | 0.380            |
| Parafovea                    | 57.68 ± 5.30                         | 57.87 ± 4.48                           | 0.769            |
| Para sup hemi                | 57.88 ± 5.35                         | 58.51 ± 4.18                           | 0.496            |
| Para inf hemi                | 57.23 ± 4.90                         | 57.49 ± 5.49                           | 0.916            |
| Para superior                | 57.11 ± 6.23                         | 58.46 ± 4.20                           | 0.264            |
| Para nasal                   | 58.45 ± 4.44                         | 59.30 ± 5.25                           | 0.620            |
| Para inferior                | 56.45 ± 5.36                         | 57.92 ± 9.46                           | 0.602            |
| Para temporal                | 57.83 ± 5.71                         | 58.15 ± 5.31                           | 0.918            |
| Perifovea                    | 53.57 ± 7.73                         | 54.93 ± 6.05                           | 0.349            |
| Peri sup hemi                | 54.11 ± 8.22                         | 55.14 ± 6.01                           | 0.389            |
| Peri inf hemi                | 53.03 ± 7.70                         | 54.74 ± 6.39                           | 0.348            |
| Peri superior                | 53.61 ± 8.81                         | 54.37 ± 6.46                           | 0.271            |
| Peri nasal                   | 51.93 ± 8.52                         | 53.76 ± 7.17                           | 0.379            |
| Peri inferior                | 52.86 ± 8.46                         | 54.17 ± 7.22                           | 0.479            |
| Peri temporal                | 55.85 ± 7.06                         | 57.52 ± 4.95                           | 0.285            |
| <b>VD of ONH (%)</b>         |                                      |  |                  |
| wpVD (total disc)            | 49.41 ± 2.46                         | 49.42 ± 2.75                           | 0.639            |
| iVD (inside disc)            | 52.15 ± 3.84                         | 52.22 ± 5.63                           | 0.922            |
| ppVD average (peripapillary) | 51.25 ± 2.49                         | 51.36 ± 3.45                           | 0.609            |
| ppVD sup hemi                | 51.31 ± 3.75                         | 51.40 ± 2.91                           | 0.517            |
| ppVD inf hemi                | 51.12 ± 2.34                         | 51.42 ± 3.49                           | 0.736            |
| ppVD superior                | 51.07 ± 4.55                         | 51.48 ± 3.65                           | 0.432            |
| ppVD nasal                   | 48.62 ± 3.76                         | 49.19 ± 2.42                           | 0.306            |
| ppVD inferior                | 53.00 ± 3.34                         | 53.21 ± 4.69                           | 0.571            |
| ppVD temporal                | 52.10 ± 4.74                         | 53.34 ± 3.21                           | 0.467            |

VD Vessel density, SCP Superficial capillary plexus, DCP Deep capillary plexus, para parafovea, peri perifovea, sup hemi Superior hemifield, inf hemi Inferior hemifield, wpVD Whole papillary vessel density, iVD Inside disk vessel density, ppVD Peripapillary vessel density.

Bold values represent statistically significant ones.

\*Independent samples T-test.

**Table 2.** FAZ, Non-Flow and Flow Assessment Tool Parameters of OCTA.

|   | MIS-C group<br>(n = 34)<br>Mean ± SD | Control group<br>(n = 36)<br>Mean ± SD | p*               |
|---|--------------------------------------|--|------------------|
| <b>FAZ assessment tool variables</b>                    |                                      |  |                  |
| FAZ area (mm <sup>2</sup> ) in full retinal vasculature | 0.28 ± 0.10                          | 0.29 ± 0.08                            | 0.735            |
| FAZ perimeter (mm)                                      | 2.04 ± 0.35                          | 2.08 ± 0.29                            | 0.915            |
| FD-300  | 54.48 ± 5.18                         | 56.93 ± 3.84                           | <b>0.024</b>     |
| <b>Non-flow assessment tool variables</b>               |                                      |  |                  |
| FAZ area (mm <sup>2</sup> ) in SCP                      | 0.49 ± 0.12                          | 0.53 ± 0.12                            | 0.233            |
| <b>Flow assessment tool variables</b>                   |                                      |  |                  |
| Outer retina flow area (mm <sup>2</sup> )               |                                      |  |                  |
| 1 mm radius   | 0.65 ± 0.35                          | 1.22 ± 0.55                            | <b>&lt;0.001</b> |
| 2 mm radius   | 3.30 ± 1.15                          | 5.00 ± 1.80                            | <b>&lt;0.001</b> |
| 3 mm radius   | 8.79 ± 2.01                          | 10.78 ± 2.53                           | <b>0.003</b>     |
| Choriocapillaris flow area (mm <sup>2</sup> )           |                                      |  |                  |
| 1 mm radius   | 2.19 ± 0.13                          | 2.29 ± 0.10                            | <b>0.013</b>     |
| 2 mm radius   | 8.84 ± 0.51                          | 9.17 ± 0.47                            | <b>0.034</b>     |
| 3 mm radius   | 19.61 ± 3.53                         | 20.79 ± 0.82                           | 0.083            |

FAZ Foveal avascular zone, FD Foveal density, SCP Superficial capillary plexus.

Bold values represent statistically significant ones.

\*Independent samples T-test was used for comparison.

COVID-19 patients, but this did not reach statistical significance. Savastano et al. [7] found no significant difference in terms of FAZ area and FAZ perimeter in the COVID-19 group compared to the control group. In Turker et al. [16] study, FAZ area did not show a difference between the early period and 6-month after COVID-19 infection. Also, no significant difference was found in FAZ area between the patient group and the control group at either the early period or 6-month after COVID-19 infection. Our results on FAZ parameters are in line with previous studies.

Our current study further demonstrates decreased outer retina and choriocapillaris flow area. Turker et al. [16] found that CC flow area at 6-month after COVID-19 infection was significantly lower than the early period examination. However, there was no difference in CC flow area between the patient and control groups at either the early or 6-month follow-up periods after COVID-19 infection. Conversely, in another Turker et al. study [23] evaluating hospitalized COVID-19 patients, the study group had significantly higher CC flow area values than controls and this situation was attributed to reactive vasodilation response to hypoxia due to the ischemia of the choroid tissue and systemic inflammatory factors.

The SARS-CoV-2 virus enters the cell via binding to angiotensin-converting enzyme 2 (ACE2) and transmembrane serine protease 2 receptors [24]. Tissues with excess ACE2 receptors such as endothelium, lung, myocardium, intestine, and kidney are frequently affected during SARS-CoV-2 infection [25]. Especially on the endothelial cell membrane, ACE2 is the predominant receptor. Endothelial damage due to direct invasion of the virus or secondary to released cytokines plays a critical role in the inflammatory and disseminated coagulation processes during COVID-19, which results in an increased risk of thromboembolic, cardiovascular, and cerebrovascular complications in patients. Retina and CC are also highly vascularized tissues in the body. Accordingly, the effects of inflammatory and ischemic diseases could be observed in retina and choroid. Similar to COVID-19, MIS-



C is associated with prevalent microangiopathy and inflammation. Thus, it is possible to observe impairment of blood flow in retina and CC. In the present study, detection of decreased retinal VD of all segments in SCP and flow of outer retina and choriocapillaris in an otherwise healthy cohort using OCTA is quite remarkable. All participants in the study had BCVA of  $\geq 20/20$  and ocular examination was normal. Furthermore, all were completely healthy before the diagnosis of MIS-C. Therefore, these results were thought to be related to MIS-C.

Although our study is the first to evaluate retinal microcirculation in MIS-C patients, it has several limitations. First, the results of a single-centre study cannot be generalized for all MIS-C. Second, our study included a relatively small number of the cohort. Furthermore, long-term follow-up of the patients was lacking.

In conclusion, this study highlights certain aspects of MIS-C-related retinal vasculopathy. Decreased retinal vessel density and CC flow in cases of SARS-CoV-2 related MIS-C was found, which demonstrates the complexity of the disease and its multiorgan involvement. Management of SARS-CoV-2 related MIS-C should include retinal assessment, with a close follow-up. Future multi-centred, larger-scale, clinical, and experimental studies are needed to understand the exact effect of MIS-C on retinal and choroidal vasculature better and to elucidate whether these alterations have permanent and long-term effects.

## SUMMARY

### What was known before

- Endothelial injury and microvascular damage act as the originator of systemic inflammation and thrombosis in severe COVID-19.
- Studies using OCTA demonstrated impaired retinal vessel density and flow in adult COVID-19 patients.
- No studies have been conducted to evaluate retinal and choroidal microcirculation in MIS-C patients by now.

### What this study adds

1. Multisystem Inflammatory Syndrome in Children (MIS-C) group showed decreased vessel density in superficial capillary plexus and foveal density (FD-300) compared to healthy controls.
2. MIS-C related decreased flow in outer retina and choriocapillaris layer was observed.

## DATA AVAILABILITY

The datasets generated during and/or analysed during the current study are available from the corresponding author on reasonable request.

## REFERENCES

1. Ramcharan T, Nolan O, Lai CY, Prabhu N, Krishnamurthy R, Richter AG, et al. Paediatric inflammatory multisystem syndrome: Temporally associated with SARS-CoV-2 (PIMS-TS): Cardiac features, management and short-term outcomes at a UK tertiary paediatric hospital. *Pediatr Cardiol*. 2020;41:1391–401.
2. McMurray JC, May JW, Cunningham MW, Jones OY. Multisystem Inflammatory Syndrome in Children (MIS-C), a Post-viral myocarditis and systemic vasculitis-A critical review of its pathogenesis and treatment. *Front Pediatr*. 2020;8:626182. 16
3. Lo TC, Chen YY. Ocular and systemic manifestations in paediatric multisystem inflammatory syndrome associated with COVID-19. *J Clin Med*. 2021;10:2953.
4. Fraser DD, Patterson EK, Daley M, Cepinskas G. Case Report: Inflammation and endothelial injury profiling of COVID-19 pediatric Multisystem Inflammatory Syndrome (MIS-C). *Front Pediatr*. 2021;9:597926.

5. Spaide RF, Fujimoto JG, Waheed NK, Sadda SR, Staurengi G. Optical coherence tomography angiography. *Prog Retin Eye Res*. 2018;64:1–55.
6. de Carlo TE, Romano A, Waheed NK, Duker JS. A review of optical coherence tomography angiography (OCTA). *Int J Retin Vitreous*. 2015;1:5.
7. Savastano MC, Gambini G, Cozzupoli GM, Crincoli E, Savastano A, De Vico U, et al. Against COVID-19 Post-acute care study group. Retinal capillary involvement in early post-COVID-19 patients: A healthy controlled study. *Graefes Arch Clin Exp Ophthalmol*. 2021;259:2157–65.
8. Abrishami M, Emamverdian Z, Shoeibi N, Omidtabrizi A, Daneshvar R, Saeidi Rezvani T, et al. Optical coherence tomography angiography analysis of the retina in patients recovered from COVID-19: A case-control study. *Can J Ophthalmol*. 2021;56:24–30.
9. Hohberger B, Ganslmayer M, Lucio M, Kruse F, Hoffmanns J, Moritz M, et al. Retinal microcirculation as a correlate of a systemic capillary impairment after severe acute respiratory syndrome coronavirus 2 infection. *Front Med (Lausanne)*. 2021;8:676554. 9
10. Multisystem inflammatory syndrome in children (MIS-C) associated with coronavirus disease 2019 (COVID-19) (2020). <https://emergency.cdc.gov/han/2020/han00432.asp>. Accessed 14 May 2020
11. Multisystem inflammatory syndrome in children and adolescents temporally related to COVID-19 (2020). <https://www.who.int/news-room/commentaries/detail/multisystem-inflammatory-syndrome-in-children-and-adolescents-with-covid-19>. Accessed 15 May 2020
12. Varga Z, Flammer AJ, Steiger P, Haberecker M, Andermatt R, Zinkernagel AS, et al. Endothelial cell infection and endotheliitis in COVID-19. *Lancet (Lond, Engl)*. 2020;395:1417–8.
13. Lowenstein CJ, Solomon SD. Severe COVID-19 is a microvascular disease. *Circulation* 2020;142:1609–11.
14. Marchetti M. COVID-19-driven endothelial damage: Complement, HIF-1, and ABL2 are potential pathways of damage and targets for cure. *Ann Hematol*. 2020;99:1701–7.
15. Zapata MÁ, Banderas García S, Sánchez-Moltalvá A, Falcó A, Otero-Romero S, Arcos G, et al. Retinal microvascular abnormalities in patients after COVID-19 depending on disease severity. *Br J Ophthalmol*. 2020;16:bjophthalmol-2020-317953.
16. Turker IC, Dogan CU, Dirim AB, Guven D, Kutucu OK. Evaluation of early and late COVID-19-induced vascular changes with optical coherence tomography angiography. *Can J Ophthalmol*. 2021;21:S0008-4182(21)00171-X.
17. Cennamo G, Reibaldi M, Montorio D, D'Andrea L, Fallico M, Triassi M. Optical coherence tomography angiography features in Post-COVID-19 pneumonia patients: A pilot study. *Am J Ophthalmol*. 2021;227:182–90.
18. González-Zamora J, Bilbao-Malavé V, Gándara E, Casablanca-Piñera A, Boquera-Ventosa C, Landecho MF, et al. Retinal microvascular impairment in COVID-19 bilateral pneumonia assessed by optical coherence tomography angiography. *Biomedicines* 2021;9:247.
19. Ashraf M, Sampani K, Clermont A, Abu-Qamar O, Rhee J, Silva PS, et al. Vascular density of deep, intermediate and superficial vascular plexuses are differentially affected by diabetic retinopathy severity. *Invest Ophthalmol Vis Sci*. 2020;61:53.
20. Coscas F, Glacet-Bernard A, Miere A, Caillaux V, Uzzan J, Lupidi M, et al. Optical coherence tomography angiography in retinal vein occlusion: Evaluation of superficial and deep capillary plexa. *Am J Ophthalmol*. 2016;161:160–71.e1-2.
21. Khairallah M, Abroug N, Khohtali S, Mahmoud A, Jelliti B, Coscas G, et al. Optical coherence tomography angiography in patients with behçet uveitis. *Retina* 2017;37:1678–91.
22. Savastano A, Crincoli E, Savastano MC, Younis S, Gambini G, De Vico U, et al. Peripapillary retinal vascular involvement in early post-COVID-19 patients. *J Clin Med*. 2020;9:2895.
23. Turker IC, Dogan CU, Guven D, Kutucu OK, Gul C. Optical coherence tomography angiography findings in patients with COVID-19. *Can J Ophthalmol*. 2021;6:83–87.
24. Hoffmann M, Kleine-Weber H, Schroeder S, Kruger N, Herrler T, Erichsen S, et al. SARS-CoV-2 cell entry depends on ACE2 and TMPRSS2 and is blocked by a clinically proven protease inhibitor. *Cell* 2020;181:271–80.
25. Vabret N, Britton GJ, Gruber C, Hegde S, Kim J, Kuksin M, et al. Immunology of COVID-19: Current state of the science. *Immunity* 2020;52:910–41.

## AUTHOR CONTRIBUTIONS

Conceptualization: BYT, HES; Methodology: BYT, HES; Formal analysis and investigation: BYT, KA, EZB, LK; Writing - original draft preparation: BYT, HES; Writing - review and editing: BYT, HES, BO, LK; Funding acquisition: none, Resources: none; Supervision: BYT, HES, KA, EZB, BO, LK. All authors commented on previous versions of the manuscript. All authors read and approved the final manuscript.

## COMPETING INTERESTS

The authors declare no competing interests.

### **ETHICS APPROVAL**

The study was reviewed and approved by the local ethics committee of Kocaeli University (Approval number: GOKAEK-2021/15.20).

### **ADDITIONAL INFORMATION**

**Supplementary information** The online version contains supplementary material available at <https://doi.org/10.1038/s41433-022-02081-8>.

**Correspondence** and requests for materials should be addressed to Büşra Yılmaz Tuğan.

**Reprints and permission information** is available at <http://www.nature.com/reprints>

**Publisher's note** Springer Nature remains neutral with regard to jurisdictional claims in published maps and institutional affiliations.